Roper excitation in $\vec{p} + \alpha \to \vec{p} + \alpha + X$ reactions

S. Hirenzaki

Department of Physics, Nara Women's University, Nara 630-8506, Japan

A. D. Bacher and S. E. Vigdor

Department of Physics, Indiana University, Bloomington, Indiana 47405

We calculate differential cross sections and the spin transfer coefficient D_{nn} in the $\vec{p} + \alpha \to \vec{p} + \alpha + \pi^0$ reaction for proton bombarding energies from 1 to 10 GeV and $\pi^0 - p$ invariant masses spanning the region of the $N^*(1440)$ Roper resonance. Two processes—Δ excitation in the α particle and Roper excitation in the proton—are included in an effective reaction model which was shown previously to reproduce existing inclusive spectra. The present calculations demonstrate that these two contributions can be clearly distinguished via D_{nn}, even under kinematic conditions where cross sections alone exhibit no clear peak structure due to the excitation of the Roper resonance. [S0556-2813(99)03003-4]

PACS number(s): 14.20.Gk, 25.40.−h, 13.75.−n

I. INTRODUCTION

An important goal of theoretical approaches to nonperturbative QCD is to reproduce the spectrum and properties of nucleon resonances in terms of quark and gluon constituents. Excited baryons with the same quantum numbers as the nucleon—e.g., the $N^*(1440)$ Roper resonance and the $N^*(1710)$—are particularly poorly understood at present. It has been difficult to understand in models why an excited configuration of three constituent quarks with the same quantum numbers as the nucleon would lie as low in mass as 1440 MeV [1]. This problem has opened the door to speculative alternative interpretations of the structure of the Roper resonance, e.g., involving collective excitations of the nucleon [2] or hybrid states with more valence constituents than three quarks [3]. Tests of such structure models have been impeded by experimental difficulties in exciting the Roper selectively.

Recent experiments at the Laboratoire National Saturne [4] have provided encouraging signs that the (α, α') reaction on the proton may provide a method for such selective excitation. Two distinct peaks observed in small-angle inclusive α-particle inelastic scattering spectra at $T_\alpha = 4.2$ GeV were interpreted as arising, respectively, from Δ excitation in the α projectile (DEP) and Roper excitation in the proton target [4]. A subsequent theoretical analysis [5] demonstrated that this picture is indeed qualitatively consistent with the measured inclusive spectra. The above two mechanisms, illustrated in Fig. 1, were shown [5] to dominate over other possible mechanisms, such as Roper excitation in the projectile or excitation of two Δ particles. However, it was also found that the interference between the two mechanisms in Fig. 1 is appreciable and necessary to consider for a quantitative account of the data. In other work [6], the identification of the second observed peak in α-p inelastic scattering as arising entirely from the Roper resonance has been called into question, on the basis of multipole decompositions of a high statistics sample of events from the $K^- p \to K^- p \pi^+ \pi^-$ reaction.

It is thus interesting to consider, within the framework of the same reaction model [5], whether other experiments in the p-α system may exhibit enhanced sensitivity to the Roper excitation amplitudes. For example, it was subsequently predicted [7] that the signal for Roper excitation should be strongly enhanced with respect to the DEP background in $p(\alpha, \alpha')$ reactions by raising the α-particle bombarding energy to 10–15 GeV. In the present paper, we demonstrate the value of *polarization transfer* measurements in exclusive $\vec{p} + \alpha \to \vec{p} + \alpha + X$ reactions for distinguishing the Roper (isoscalar, non-spin-flip) excitation from Δ (isovector, spin-flip) excitation. The utility of polarization transfer measurements for distinguishing analogous *nuclear* transitions has been clearly demonstrated in medium-energy proton-nucleus reaction studies [8].

In the present case, if the reaction proceeds through an intermediate Δ, we expect a negative value $D_{nn} < 0$ for the transfer of normal polarization from the incident proton to the final-state proton [9], in analogy with the results for Gamow-Teller transitions in nuclei with $A(\vec{p}, \vec{n})$ reactions at moderate momentum transfer [10]. In contrast, the simple spin structure for the direct excitation of the Roper by an α particle, $0^+ + \frac{1}{2}^+ \to 0^+ + \frac{1}{2}^+$, requires $D_{nn} = 1$ by parity conservation [11–13]. Furthermore, for the Roper decay mode $N^* \to N + \pi$, the polarization of the Roper is completely transferred to its daughter proton when the proton is emitted along the Roper polarization axis in the Roper rest frame. Thus, for a restricted region of phase space in a coincidence measurement $\vec{p} + \alpha \to \vec{p} + \alpha + X$, one can expect to distinguish the Roper contribution from the Δ contribution by observing D_{nn}, even if one does not see a clear peak in cross section spectra. These ideas have been described previously [9], but only in a qualitative manner.

In the present work, we carry out quantitative calculations for differential cross sections and D_{nn} in the exclusive $\vec{p} + \alpha \to \vec{p} + \alpha + \pi^0$ reaction at several bombarding energies, including both mechanisms in Fig. 1. In our model, we include proton-α distortions using a spin-independent eikonal approximation. We expect this model to be reasonably good for predicting cross sections and D_{nn}, since the D_{nn} value
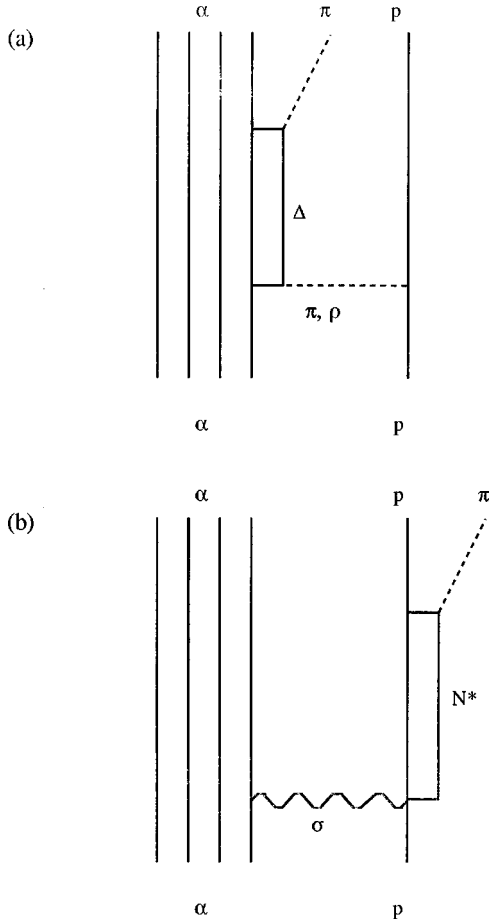
FIG. 1. Diagrams for the $\vec{p} + \alpha \rightarrow \vec{p} + \alpha + X$ reactions considered in this paper. They are (a) the Δ excitation in the α [14] and (b) the Roper excitation in the proton [5]. The σ exchange must be interpreted as an effective interaction in the isoscalar exchange channel [5].

for Roper excitation is fixed by parity conservation, independent of distortions and other details of the production mechanism. On the other hand, this simple treatment of distortions may be inadequate for other, less robust spin observables, such as the analyzing power A_y.

The paper is organized as follows. Section II describes the theoretical model for the $\vec{p} + \alpha \rightarrow \vec{p} + \alpha + X$ reactions. Section III presents the numerical results of the reaction model. Section IV summarizes the results and indicates possible applications of this technique to other nucleon excitations.

II. MODEL FOR THE $\vec{p} + \alpha \rightarrow \vec{p} + \alpha + X$ REACTIONS

We use the same model developed in Refs. [5,7,14] and refer the reader to these references for details. We include the two dominant processes shown in Fig. 1—Δ excitation in the α-particle and Roper excitation in the proton—which are necessary to reproduce the inclusive cross section spectra from Ref. [4]. We can write the amplitudes as

$$-iT^{\Delta}_{m'm} = -\frac{16}{9} F_\alpha \left(\frac{f^*}{\mu}\right)^2 \left(\frac{f}{\mu}\right) G_\Delta \sqrt{\frac{-q^2}{\vec{q}^2_\Delta}} [(V_{l'} - V_{t'})$$

$$\times (\vec{p}_\Delta \cdot \hat{q}_\Delta) \hat{q}_N + V_{t'} \vec{p}_\Delta] \cdot \langle m' | \vec{\sigma} | m \rangle \quad (1)$$

and

$$-iT^*_{m'm} = -4F_\alpha \left(\frac{f'}{\mu}\right) G_* g_{\sigma NN*} D_\sigma F^2_\sigma g_{\sigma NN} \vec{p}_* \cdot \langle m' | \vec{\sigma} | m \rangle, \quad (2)$$

where G_Δ and G_* are the propagators of the Δ and Roper resonances, D_σ is the propagator of the σ meson, F_α is the ^{4}He nuclear form factor, μ is the pion mass, and F_σ is the σNN vertex form factor. $V_{l'}$ and $V_{t'}$ stand for the longitudinal and transverse parts of the $NN \rightarrow N\Delta$ effective interaction which includes π, ρ, and g' contributions. The f's and g's in Eqs. (1) and (2) are coupling constants. In particular, f' is determined to reproduce the decay width of the $N^*(1440) \rightarrow \pi N$ channel. All details, including parameter values, are given in Refs. [5,14]. In Eqs. (1) and (2), the subscripts on momenta, Δ, N, and *, indicate the coordinate system where the momenta are to be evaluated: the Δ rest frame, the initial proton rest frame, and the Roper rest frame, respectively. The magnetic quantum numbers m and m' for initial and final protons refer to a spin quantization axis perpendicular to the reaction plane formed by the beam and outgoing proton or N^* directions.

In the amplitudes we include only $p + \alpha + \pi^0$ as the final state. In p-α coincidence experiments, the missing mass of the π^0 can be reconstructed to eliminate contributions from 2π decay channels of the Roper resonance. However, their neglect in the calculations reported here for inclusive spectra is expected to yield an underestimate of the cross section for the Roper process in the higher-excitation-energy region of the inclusive spectra. The 2π decay channels mainly contribute to the inclusive cross section at higher excitation energy because of the larger available phase space. They will make the Roper contribution to inclusive spectra broader than shown here, especially at the higher incident energies [7].

The nuclear form factor F_α contained in Eqs. (1) and (2) is defined as

$$F_\alpha(\vec{k}) = \frac{1}{4} \int d^3 r \rho_\alpha(\vec{r}) \exp\left[-\frac{1}{2} \int_{-\infty}^{\infty} \sigma_{NN} \rho_\alpha(\vec{b}, z') dz' \right] e^{i\vec{k}\cdot\vec{r}}$$

$$\times \exp\left[-\frac{i}{2} \int_0^\infty \frac{1}{p_\pi} \Pi(p_\pi, \rho_\alpha(\vec{r}')) dl \right], \quad (3)$$

where

$$\vec{r}' = \vec{r} + \frac{\vec{p}_\pi}{|\vec{p}_\pi|} l,$$

$$\vec{k} = \vec{p}_\alpha - \vec{p}_{\alpha'}, \quad (4)$$

and $\vec{b}$ is the impact parameter. We write $F_\alpha(\vec{k})$ normalized to unity at $\vec{k} = 0$ and in the absence of distortion, as is usually done. The momenta $\vec{p}_\alpha, \vec{p}_{\alpha'}, \vec{p}_\pi$ appearing in Eqs. (3) and (4) are evaluated in the frame where the initial α particle is at rest. In Eq. (3), $\rho_\alpha(\vec{r})$ is a harmonic oscillator density distribution of ^{4}He, σ_{NN} is the nucleon-nucleon total cross section and $\Pi(p_\pi, \rho)/2\omega_\pi$ is the pion nuclear optical potential with the relativistic pion energy ω_π. In this definition of the $F_\alpha(\vec{k})$, we apply the eikonal approximation, which is known
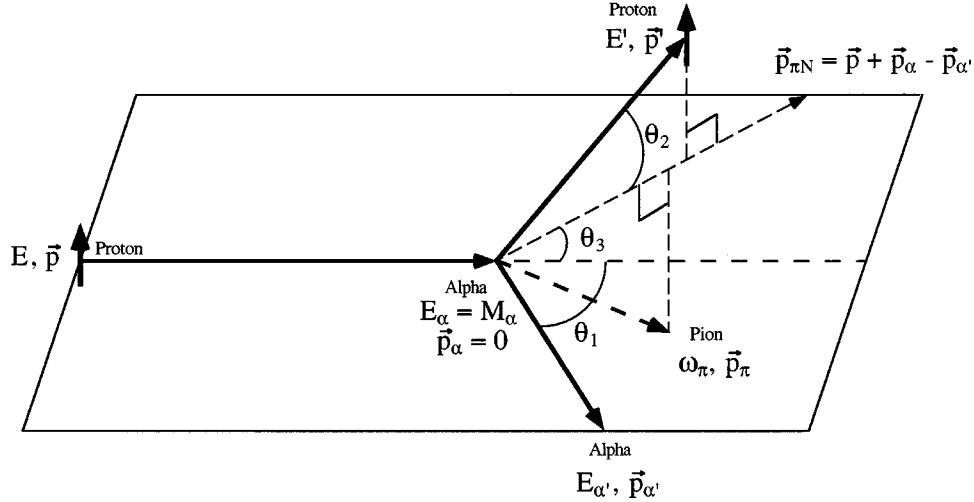
FIG. 2. Definitions of the kinematical variables used in this paper. The scattering plane is determined by $\vec{p}$ and $\vec{p}_{\alpha'}$. As indicated in this figure, $\vec{p}_{\pi N}$ is in the plane, while $\vec{p}'$ and $\vec{p}_{\pi}$ can be out of the plane. The incident proton polarization is perpendicular to the plane. Definitions of the scattering angles are also shown.

to be a good approximation at intermediate energies, to evaluate distortion effects. In addition, we neglect nonlocality due to meson exchange, and also the propagation of Δ and N^*, because of their large widths and prompt decay.

The observed inclusive cross sections led the authors of Ref. [4] to interpret the Roper resonance as the $E0$ monopole excitation of the nucleon. However, in our theoretical model, the monotonic decrease of the observed angular distribution [4] is mostly a consequence of the ^{4}He form factor and not an intrinsic property of the Roper resonance. Our calculated results reproduce the trend of all of the experimental results quite well [5] without treating the Roper as the monopole excitation of the nucleon. We think that the limited information in the data obtained so far does not allow one to extract such precise information on the structure of the Roper.

Using the amplitudes shown in Eqs. (1) and (2), the coincidence cross section can be written as

$$
\frac{d\sigma}{dE_{\alpha'}d\Omega_{\alpha'}d\Omega_{p'}}
$$

$$
= \frac{p_{\alpha'}}{(2\pi)^5}\frac{M_\alpha^2 M^2}{\lambda^{1/2}(s,M^2,M_\alpha^2)}
$$

$$
\times \frac{p'^2}{p'\omega_\pi + E'(p'-p_{\pi N}\cos\theta_2)}\overline{\sum_m}\sum_{m'}|T_{m'm}^\Delta + T_{m'm}^*|^2,
$$

$$(5)$$

where M is the nucleon mass, M_α is the mass of the ^{4}He, and $\lambda(\cdots)$ is the Kallen function, defined as

$$
\lambda(a,b,c)=a^2+b^2+c^2-2ab-2bc-2ca.
$$

All kinematical variables are evaluated in the laboratory frame and defined in Fig. 2.

The normal spin transfer coefficient D_{nn} is defined as

$$
D_{nn}=\frac{(d\sigma_{uu}+d\sigma_{dd})-(d\sigma_{ud}+d\sigma_{du})}{(d\sigma_{uu}+d\sigma_{dd})+(d\sigma_{ud}+d\sigma_{du})},
\tag{6}
$$

where the indices u and d indicate the up and down spin states of the proton in the initial and final states. Here, the cross sections $d\sigma_{m'm}$ are defined by Eq. (5) without taking the spin sum and average.

III. NUMERICAL RESULTS

We first calculate cross sections for the inclusive reaction $p+\alpha\rightarrow\alpha+X$, which is the same inclusive reaction considered in Ref. [5], except for altered kinematics. In the present case, the proton is the projectile and the recoiling α particle is observed in the final state. We use the same T matrix defined in Sec. II and the same phase factors as in Ref. [5]. Since we may also have the $n+\alpha+\pi^+$ final state in the inclusive reaction, we have multiplied by an additional isospin factor of 3 the cross sections which are obtained using the T matrix from Sec. II. We calculate the inclusive cross section $d\sigma/dE_{\alpha'}d\Omega_{\alpha'}$ as a function of $T_{\alpha'}$ at different α' angles θ_1 (see Fig. 2 for the definition of θ_1). The calculated results are shown in Figs. 3 and 4 for incident proton energies of 1 and 10 GeV. We also show the contributions to the inclusive cross section from the Roper excitation process alone.

In Fig. 3, we show the calculated results for $T_p = 1$ GeV, which corresponds to $T_\alpha = 4$ GeV in the inverse kinematics of the Saturne experiment [4]. It is interesting to compare our present results with the measurements from Saturne. The shape of the energy spectrum at $\theta_1 = 20°$ in Fig. 3(b) strongly resembles that observed in the inverse kinematics [5]. We find, however, that the angular dependence of the cross section is much milder in the present case than for the case of an α-particle projectile: in going from $\theta_1 = 0°$ to $60°$, the cross section decreases by only about a factor of 3. This mild angular dependence is due to the behavior of the α-α' transition form factor F_α in Eqs. (1) and (2). We evaluate the form factor using the momentum transfer for the α
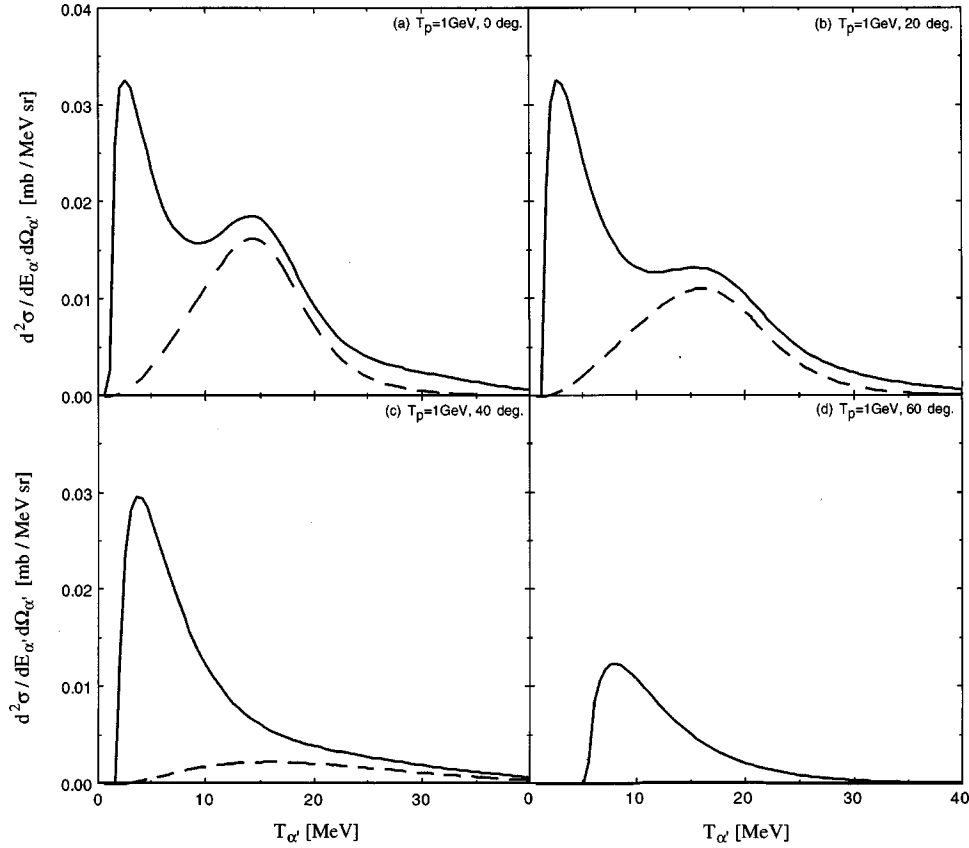
FIG. 3. Calculated energy spectrum (solid line) and contribution from Roper excitation process alone (dashed line) for the inclusive $p + \alpha \rightarrow \alpha + X$ reaction at $T_p = 1$ GeV as a function of recoil α-particle energy $T_{\alpha'}$. The recoil α angles (in degrees) in the laboratory frame correspond to values of θ_1 defined in Fig. 2, and are indicated for each spectrum.

particle in the initial α rest frame. In the present kinematics, the momentum transfer does not depend on the angle θ_1, but only on the energy $E_{\alpha'}$. Thus, F_α, which caused the steep angular dependence observed in the case of inverse kinematics, does not produce an angular dependence of the energy spectrum calculated here. The observed dependence of the spectra in Figs. 3 and 4 on θ_1 arises instead from kinematic effects described below.

In Fig. 3 we can see the cross sections from the Roper process alone at different values of θ_1 for $T_p = 1$ GeV. As θ_1 increases, the Roper peak moves to larger $T_{\alpha'}$ and becomes weaker and broader. This behavior reflects changes in the invariant mass of the final πN system. Since the invariant mass changes more slowly as a function of $T_{\alpha'}$ for larger angles, the peak position moves to larger $T_{\alpha'}$ and the peak is broader when we plot cross sections as a function of $T_{\alpha'}$. For larger $T_{\alpha'}$, the transition form factor F_α makes the Roper peak weaker. Furthermore, at $\theta_1 = 40°$ and $60°$ with $T_p = 1$ GeV, the invariant mass cannot reach 1440 MeV, so that the Roper contributions are much smaller than at more forward α-particle angles.

The contribution from the Δ process has a different angular dependence, as can be seen in Fig. 3, since the invariant mass of the Δ system is determined in a different way (see Ref. [14]). Nonetheless, the Δ peak also moves to larger $T_{\alpha'}$ for larger θ_1, and decreases in strength as a result of F_α.

For higher T_p (see Fig. 4), the Roper contribution is larger than the Δ contribution, since the Roper peak moves to

smaller $T_{\alpha'}$, where F_α is larger. This is also the case in inverse kinematics, as reported in Ref. [7]. At the same time, the Roper peak is sharper because the invariant mass changes more rapidly as a function of $T_{\alpha'}$. In the present case, however, the Roper and Δ peaks strongly overlap for higher T_p, and cannot be distinguished in inclusive spectra alone.

The angular dependence of the cross section for both the Roper and the Δ excitation processes in Fig. 4 is much flatter than at lower T_p, because of the $p_{\alpha'}$ included in the phase space factor of the cross section. The increase of $p_{\alpha'}$ at larger θ_1 overcomes the effect of F_α in this narrow energy range close to $p_{\alpha'} = 0$, making the cross section larger.

The inclusive spectra shown in Figs. 3 and 4 indicate that the α-particle recoil energy is quite small in the laboratory frame, and that good energy resolution is needed to select the portion dominated by Roper excitation. This fact favors the use of a thin, windowless gaseous ^{4}He target in an experiment. The use of a storage ring and internal target environment, as proposed in Ref. [9], seems to be most suitable to obtain sufficient luminosity.

Before presenting the numerical results for *exclusive* reactions, we need to clarify the kinematic configurations in which we calculate the exclusive cross sections. As described in Sec. I, we are interested in the restricted phase space in the final state where the spin transfer coefficient D_{nn} of the Roper process is equal to 1. In the present reaction, the energy and momentum of the Roper are determined uniquely for each final $\vec{p}_{\alpha'}$. Furthermore, the normal polarization of
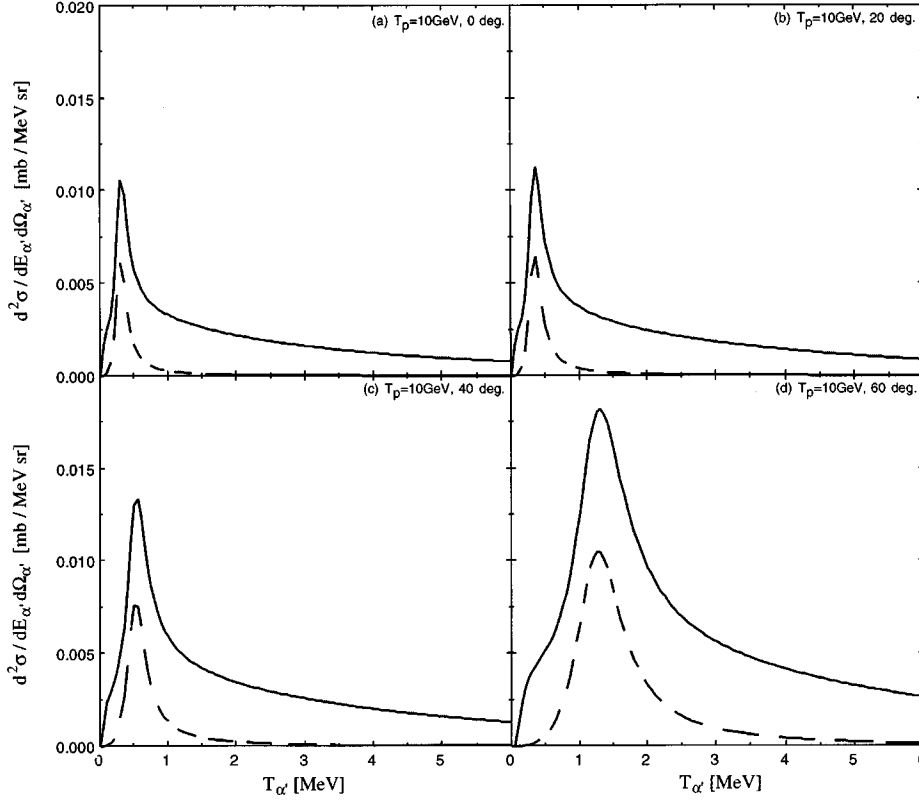
FIG. 4. Same as Fig. 3 except for $T_p = 10$ GeV.

the proton beam is transferred completely to the produced Roper. When the Roper decays into the $\pi+p$ system, we can determine the desired momenta and energies of the π and p uniquely by imposing the additional condition that the proton be emitted along the polarization axis of the Roper within the Roper rest frame. This condition guarantees full transfer of the Roper polarization to its daughter proton. The final proton energy and emission angles in the laboratory frame (see Fig. 2) are then obtained by a Lorentz transformation from the Roper rest frame to the laboratory frame. In this restricted kinematic configuration, we always get $D_{nn}=1$ for the Roper contribution. As an example, Fig. 5 shows, for the case of $T_p=2$ GeV, the final proton emission angles (θ_2,θ_3) and kinetic energies as a function of $T_{\alpha'}$ for several values of θ_1. All of our results for the exclusive reaction are obtained in this kinematic condition. Thus, the final proton energy and angles in the laboratory frame vary with those of the final α, so as to satisfy the conditions described above. Note, however, from Fig. 5 that the final proton remains less than 20° out of plane ($\theta_2 < 20°$) over the entire range of interest, so that its polarization is always predominantly transverse to its motion in the laboratory frame. Furthermore, the decay proton energies in the laboratory frame are in a range near that where high-figure-of-merit proton polarimeters have already been developed at LAMPF [15].

Experiments will, of course, average over finite angular and energy acceptances for the decay proton. Thus, we have also considered final protons emitted at nonzero angles from the polarization axis in the Roper rest frame. We find, for example, that in the $T_p=2$ GeV, $\theta_1=20°$ case, one maintains $D_{nn}>0.95$ for the Roper process at its peak if decay

protons are detected over a $\pm0.5°$ angular and ±25 MeV energy range in the laboratory, centered around the optimum values.

In Figs. 6 and 7 we show the calculated exclusive reaction cross sections and the spin transfer coefficient [defined in Eqs. (5) and (6)], for $T_p=1$ GeV. Since the phase space factor of Eq. (5) diverges at the threshold for one pion production, the total cross sections are larger at smaller $T_{\alpha'}$. At the threshold, D_{nn} for the Δ process is -1 since both the proton and the pion in the final state are in the scattering plane, so that the momentum transfer to the nucleon is perpendicular to the spin polarization. D_{nn} for the Roper process is always 1 in the kinematic configuration described above. The D_{nn} associated with the interference between the two contributions is also always 1, because the interference makes a finite contribution only when the amplitude for the Roper process is nonzero. In Fig. 6, where $\theta_1=20°$, we see that the calculated cross section does not exhibit a clear peak due to the Roper contribution, but rather only a shoulder. Nonetheless, in the spin transfer coefficient one sees a clear indication of the Roper excitation process: D_{nn} clearly changes from negative to positive (~1) in the energy region where the Roper contribution becomes dominant. This feature allows the Roper contribution to be identified even without a clear corresponding peak in the cross section. It is interesting to note the very different D_{nn} behavior in Fig. 7 for $\theta_1=60°$, where the Roper process provides a minor contribution over the entire $T_{\alpha'}$ range.

Figure 8 shows results for $T_p=2$ GeV and $\theta_1=20°$. Here, Roper excitation is manifested clearly in both the cross
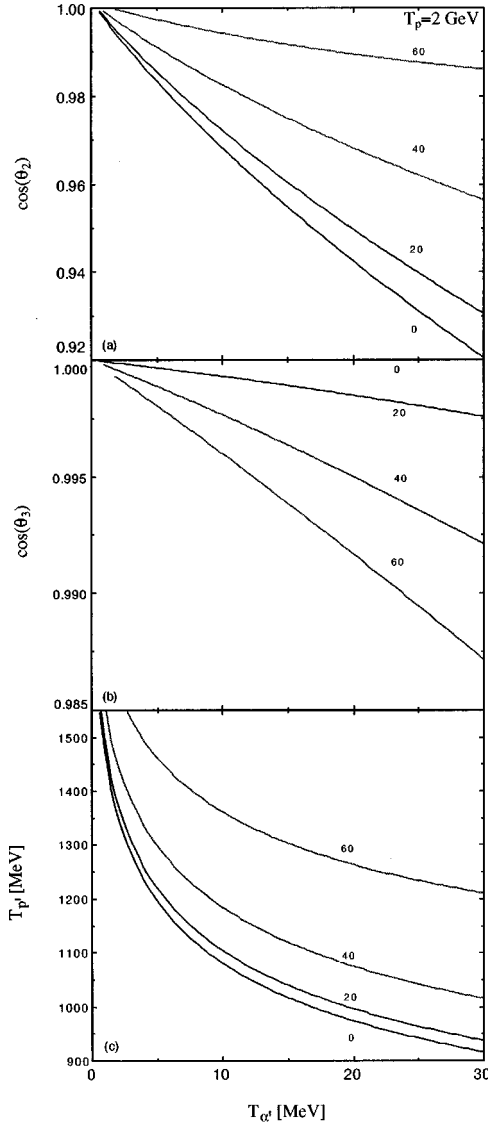
FIG. 5. Final proton emission angles (a) $\cos(\theta_2)$, (b) $\cos(\theta_3)$, and (c) final proton kinetic energies as a function of the final α-particle kinetic energy $T_{\alpha'}$ for $T_p = 2$ GeV. The curves correspond to different scattering angles of the α, θ_1, in the laboratory frame in units of degrees. See Fig. 2 for a definition of the scattering angles.

sections and D_{nn}. Figure 9 reveals the real utility of the D_{nn} signature, unveiling a Roper contribution at relatively high $T_{\alpha'}$, where the net cross section is smooth and monotonically decreasing.

In Figs. 10 and 11, we show the results for a much higher energy, $T_p = 10$ GeV. In these figures we can see that D_{nn} reaches a maximum value around the peak of the Roper contribution, before decreasing toward higher $T_{\alpha'}$, because the Δ contribution has a longer tail in the cross section than the Roper contribution. In such situations, D_{nn} measurements may yield information on the $T_{\alpha'}$ dependence of the contributing production processes far from the regions where they are kinematically maximized.

IV. SUMMARY

We have studied Roper resonance excitation in both the inclusive $p + \alpha \rightarrow \alpha + X$ reaction and the exclusive $\vec{p} + \alpha$ $\rightarrow \vec{p} + \alpha + X$ reactions at $T_p = 1-10$ GeV. We have used a reaction model developed previously to understand existing inclusive cross section measurements. The model includes the Δ excitation process in the α particle as well as the Roper excitation process in the proton. We have calculated the differential cross sections and the normal spin transfer coefficient D_{nn} for various energies and angles of the recoil α particle.

The inclusive reaction sometimes exhibits a peak from the Roper resonance excitation. The magnitude of the cross section does not have a strong dependence on the recoil α angle, in contrast to the case with inverse kinematics, since the momentum transfer to the α particle does not depend on its recoil angle. Instead, the shape and strength of the Roper contribution to the inclusive spectrum depend on the recoil α angle because of its kinematic implications for the invariant mass of the final πN system.

In the exclusive $\vec{p} + \alpha \rightarrow \vec{p} + \alpha + X$ reactions, we have calculated both the cross section and the spin transfer coefficient. The simple spin coupling for Roper production dictates that the incident proton's polarization normal to the production plane will be transferred completely to the N^*. In the restricted part of phase space described in Sec. III, we have consequently found that the spin transfer coefficient clearly shows the contribution from the Roper excitation process even when there is no corresponding peak structure in the cross section. By observing D_{nn}, one can distinguish the Roper process from the Δ background even when the energy spectrum is rather flat. We conclude that the spin transfer coefficient is a robust observable for identifying the Roper contribution.

If the polarization transfer measurements proposed here were to confirm the dominance of Roper excitation in $p + \alpha$ collisions under appropriate kinematic conditions, then coincidence experiments with polarized beams offer several potential advantages over other methods for determining so far rather poorly known properties of the Roper resonance. By changing the proton bombarding energy and the α-particle recoil angle, one can vary the invariant mass of the excited nucleon independently of the momentum transfer to the α particle. In this way, one can measure the resonance shape and improve upon existing determinations of its mass and width. Furthermore, the *a priori* knowledge of the N^* polarization will help to determine the relative branching ratios for decay channels other than πN. For example, by gating on $p + \alpha$ missing mass one could selectively study the $N\pi\pi$ channels, which are known to have substantial contributions from $\Delta\pi$, $N\rho$, and $N(\pi\pi)_{s\text{-wave}}$ intermediate states. The different intermediate states have different spin coupling and hence different characteristic spin transfers from N^* to daughter N. Measurement of the polarization transfer from incident to final proton, as a function of the reconstructed emission angle in the N^* rest frame, could then allow an improved decomposition of the $\pi\pi$ channel strength. The coupling strength of the N^* to these various channels is essential information for constraining theoretical models of the Roper structure.
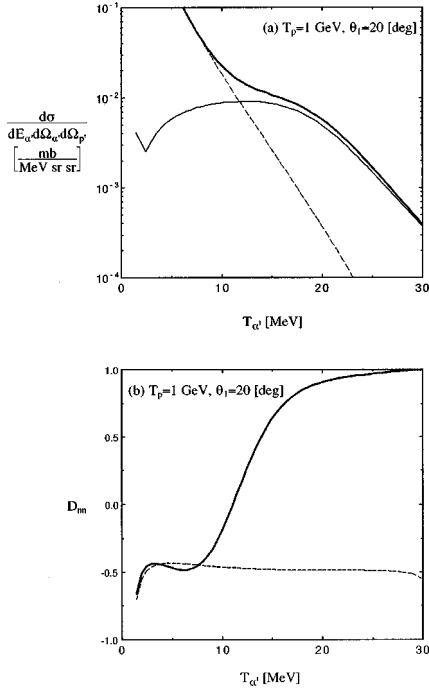
FIG. 6. (a) Differential cross section and (b) spin transfer coefficient D_{nn} of the $\vec{p}+\alpha\rightarrow\vec{p}+\alpha+X$ reaction as a function of the recoil α-particle kinetic energy $T_{\alpha'}$ at $T_p=1$ GeV and $\theta_1=20°$. The dashed, solid, and thick solid lines show the results of the Δ process, the Roper process, and the combination of the two (including the interference).

At the higher bombarding energies considered here, it is of course also possible to produce heavier baryon resonances, which have not been included in the present calculation. The cross sections for such production processes may also be sizable, since for low α-particle kinetic energies, the
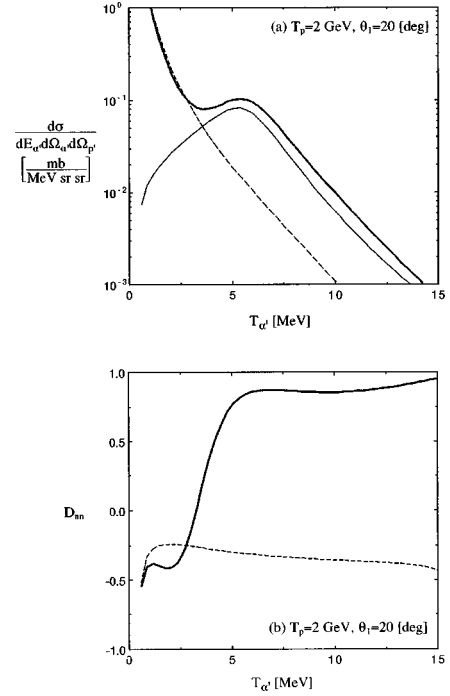
FIG. 8. Same as Fig. 6 except for $T_p=2$ GeV and $\theta_1=20°$.

α-particle form factor does not suppress the cross section. There are also possibilities to use the same kind of spin filtering for certain heavier resonances as applied to the Roper resonance in the present case. In particular, similar parity constraints on D_{nn} to N^* resonances, produced in exclusive $p+\alpha$ reactions, exist whenever the spin and parity of the resonances are $\frac{1}{2}^+$ ($D_{nn}=+1$) or $\frac{1}{2}^-$ ($D_{nn}=-1$). Furthermore, the full polarization transfer to the daughter baryon, when it is emitted along the resonance's spin quantization axis, applies equally well to $p+\pi$, $p+\eta$, and $\Lambda+K$ final
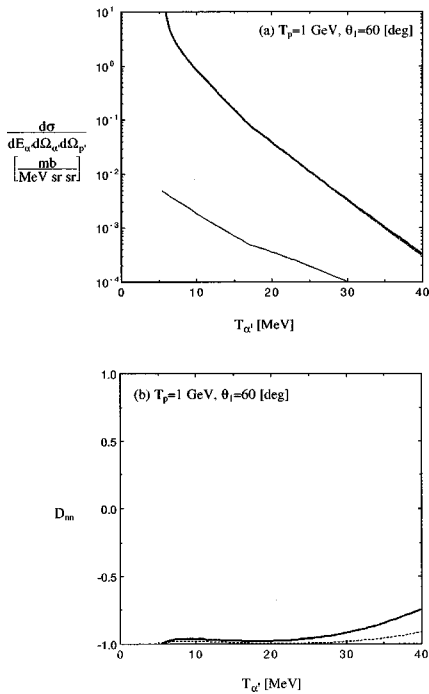

FIG. 7. Same as Fig. 6 except for $T_p=1$ GeV and $\theta_1=60°$.

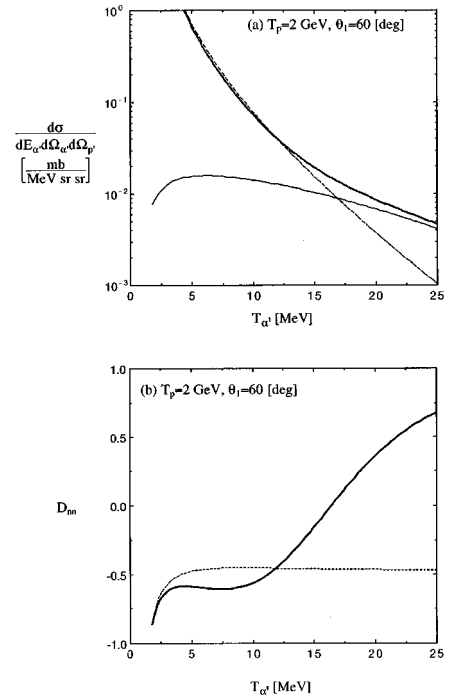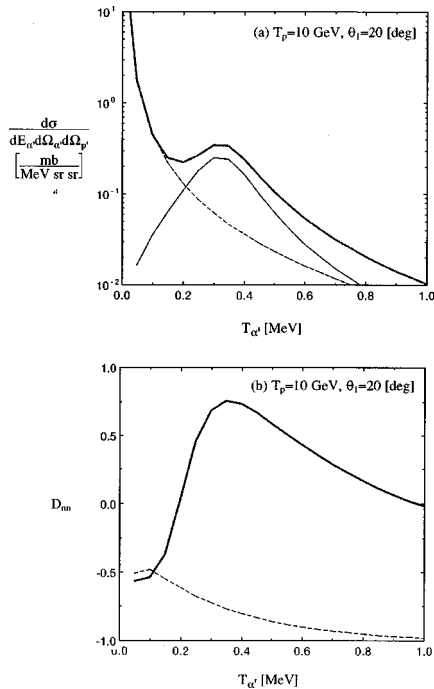FIG. 9. Same as Fig. 6 except for $T_p=2$ GeV and $\theta_1=60°$.

FIG. 10. Same as Fig. 6 except for $T_p = 10$ GeV and $\theta_1 = 20°$.

FIG. 11. Same as Fig. 6 except for $T_p = 10$ GeV and $\theta_1 = 60°$.

states. In the latter case [relevant, for example, in the $N^*(1710)$ decay], the polarization of the daughter baryon can be readily measured via the Λ's subsequent self-analyzing decay to $p\pi^-$. Thus, polarization transfer measurements in multi-GeV $p + \alpha$ collisions may help in the search for $\frac{1}{2}^+$ and $\frac{1}{2}^-$ strengths in the nucleon resonance continuum.

ACKNOWLEDGMENTS

[1] P. Stoler, Phys. Rep. **226**, 103 (1993).

[2] R. Bijker, F. Iachello, and A. Leviatan, Phys. Rev. C **54**, 1935 (1996).

[3] Z. Li, V. Burkert, and Zh. Li, Phys. Rev. D **46**, 70 (1992).

[4] H. P. Morsch et al., Phys. Rev. Lett. **69**, 1336 (1992).

[5] S. Hirenzaki, P. Fernandez de Cordoba, and E. Oset, Phys. Rev. C **53**, 277 (1996).

[6] J. Napolitano, J. Cummings, and M. Witkowski, in Proceedings of the 7th International Symposium on Meson-Nucleon Physics and the Structure of the Nucleon (MENU97), TRIUMF Report No. TRI-97-1, Vancouver, BC, Canada, 1997, p. 276.

[7] S. Hirenzaki, E. Oset, and P. Fernandez de Cordoba, Phys. Lett. B **378**, 29 (1996).

[8] J. M. Moss, Phys. Rev. C **26**, 727 (1982).

[9] Physics Motivations and Accelerator Design Concept for a Light-Ion Spin Synchrontron, IUCF Internal Report, Indiana University, 1996; S. E. Vigdor, Nucl. Phys. **A626**, 141c (1997).

[10] T. N. Taddeucci et al., Phys. Rev. Lett. **52**, 1960 (1984).

[11] P. L. Csonka, M. J. Moravcsik, and D. Scadron, Phys. Rev. **143**, 1324 (1966).

[12] P. L. Csonka and M. J. Moravcsik, Phys. Rev. **152**, 1310 (1966).

[13] H. A. Weidenmüller, in Proceedings of the International Symposium on Polarization Phenomena in Nuclear Reactions, edited by H. H. Barschall and W. Haeberli (The University of Wisconsin Press, Madison, 1970).

[14] P. Fernández de Córdoba, E. Oset, M. J. Vicente-Vacas, Yu. Ratis, J. Nieves, B. López-Alvaredo, and F. Gareef, Nucl. Phys. **A586**, 586 (1995).

[15] J. B. McClelland et al., Technical Report No. LA-UR-84-1671, Los Alamos National Laboratory, 1984.